Accepted Manuscript

Folic acid conjugates with photosensitizers for cancer targeting in photodynamic therapy: synthesis and photophysical properties

Aurélie Stallivieri, Ludovic Colombeau, Gulim Jetpisbayeva, Albert Moussaron, Bauyrzhan Myrzakhmetov, Philippe Arnoux, Samir Acherar, Régis Vanderesse, Céline Frochot

PII: S0968-0896(16)30911-7
DOI: http://dx.doi.org/10.1016/j.bmc.2016.10.004
Reference: BMC 13331

To appear in: *Bioorganic & Medicinal Chemistry*

Received Date: 27 July 2016
Revised Date: 14 September 2016
Accepted Date: 6 October 2016

Please cite this article as: Stallivieri, A., Colombeau, L., Jetpisbayeva, G., Moussaron, A., Myrzakhmetov, B., Arnoux, P., Acherar, S., Vanderesse, R., Frochot, C., Folic acid conjugates with photosensitizers for cancer targeting in photodynamic therapy: synthesis and photophysical properties, *Bioorganic & Medicinal Chemistry* (2016), doi: http://dx.doi.org/10.1016/j.bmc.2016.10.004

Graphical Abstract

Folic acid conjugates with photosensitizer for cancer targeting in photodynamic therapy: synthesis and photophysical properties

Leave this area blank for abstract info.

Aurélie Stallivieri, Ludovic Colombeau, Gulim Jetpisbayeva, Albert Moussaron, Bauyrzhan Myrzakhmetov, Philippe Arnoux, Samir Acherar, Régis Vanderesse and Céline Frochot

[a] *LRGP, UMR-CNRS 7274, and* [b] *LCPM, UMR-CNRS 7375, Lorraine-Université, 1 rue Grandville, BP 20451, 54001 Nancy Cedex, France*

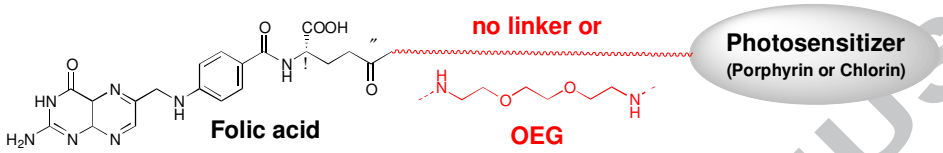

Bioorganic & Medicinal Chemistry
journal homepage: www.elsevier.com

Folic acid conjugates with photosensitizers for cancer targeting in photodynamic therapy: synthesis and photophysical properties

Aurélie Stallivieri[a], Ludovic Colombeau[a], Gulim Jetpisbayeva[a], Albert Moussaron[a], Bauyrzhan Myrzakhmetov[a], Philippe Arnoux[a], Samir Acherar[b], Régis Vanderesse[b] and Céline Frochot[a,*]

[a] *Laboratoire Réactions et Génie des Procédés, UMR-CNRS 7274, Lorraine-Université, 1 rue Grandville, BP 20451, 54001 Nancy Cedex, France*
[b] *Laboratoire de Chimie Physique macromoléculaire, UMR-CNRS 7375, Lorraine-Université, 1 rue Grandville, BP 20451, 54001 Nancy Cedex, France*

ARTICLE INFO

Article history:
Received
Received in revised form
Accepted
Available online

Keywords:
Cancer targeting
Folic acid
Photodynamic therapy
Singlet oxygen
Photosensitizers

ABSTRACT

Recent researches in photodynamic therapy have focused on novel techniques to enhance tumour targeting of anticancer drugs and photosensitizers. Coupling a photosensitizer with folic acid could allow more effective targeting of folate receptors which are over-expressed on the surface of many tumour cells. In this study, different folic acid-OEG-conjugated photosensitizers were synthesized, characterized and their photophysical properties were evaluated. The introduction of an OEG does not significantly improve the hydrophilicity of the FA-porphyrin. All the FA-targeted photosensitizers present good to very good photophysical properties. The best one appears to be Ce6. Molar extinction coefficient, fluorescence and singlet oxygen quantum yields were determined and were compared to the corresponding photosensitizer alone.

1. Introduction

Photodynamic therapy (PDT) combines a photoactivable molecule - the photosensitizer (PS) - with oxygen and light. When photosensitizers are exposed to light of a specific wavelength, the PS is promoted to an excited singlet state then to an excited triplet state that can transfer energy to oxygen, to form singlet oxygen. Singlet oxygen is highly reactive, toxic and can react with various cellular constituents causing cell damage and death.

Specific targeting of therapeutic agents to human tissues, regardless of the application fields, remains a challenge for biologists and chemists. These agents must avoid biological changes leading to rapid elimination from the body and, at the cellular level, the active molecules must distinguish different types of cells, be internalized by passing through membranes and reach their target, while phenomena resistances encountered in tumor cells, must be bypassed. Many researches' have been undertaken to improve the selectivity between different types of cells, to increase the bioavailability or give better properties of penetration into cells. For cancer treatment, these strategies can be summarized in two approaches, passive targeting and active targeting, which are sometimes combined to increase efficiency. Passive targeting focuses on the physiological differences between normal and tumor environments. Tumor tissues possess vasculature with a permeability and increased retention, leading to greater accumulation of nutrients necessary for angiogenesis. This property is called 'enhanced permeability and retention "(EPR). [1]Passive targeting of tumor cells by PDT is to vectorize PSs through different formulation systems facilitating transport and incorporation into cancer cells. Several types of vectors can be used: liposomes, nanoparticles and micellar systems. [1]

A strategy for improving the efficiency of PDT is to increase the selectivity towards tumour cells in order to reduce the adverse side-effects caused by normal cell injury. Active targeting is based on the interaction of a vector with a cell surface marker (receptor or antigen) which is over-expressed onto tumour cells. Among the tumour targeting agents, numerous biomolecules have been studied. These include peptides,[2-4] lipoproteins,[5, 6] saccharides[7] or antibodies.[8] Folic acid (FA)

is also a targeting agent which has been widely studied in the field of imaging or diagnostics[9-11] and for the treatment of certain cancers.[2, 3, 12, 13][1]

Numerous cancer cell lines over-express FA receptors because of their fast growth and cell division.[14] Indeed, the folate receptors (FRs) are over-expressed on prostate, brain, lung, nose, ovary, colon, cancer cells[9, 10] and have very low expression on normal cells.[15] This selective over-expression makes FRs interesting tumour targets when FA is conjugated to anticancer molecules.[16]

By attaching a PS to FA, in 2005 our team demonstrated the selectivity of the targeted PS for the first time.[17] Since this study, other groups have shown the potential effectiveness of FA for tumour-specific drug delivery in the PDT field. Among the different carriers of folate are nanoparticles,[2, 18-22] liposomes,[6, 23, 24] micelles,[25, 26] quantum dots[27-29] or carbon nanotubes and other nanocomposites.[22, 30-33] Some studies have focused on the PS conjugation to FA *via* a spacer. The linker is often a polyethylene glycol (PEG) arm of variable length.[34-37] Stefflova et al. were the first to design folate targeted photosensitizers using a peptide sequence as stable linker between FA and PS.[38] More recently, directly linked FA-PS molecules were synthesized.[39, 40] In a recent review we collected the data concerning the use of FA for PDT applications from the literature.[41]

We chose two different classes of PS: "synthetic" PSs i.e. a porphyrin and a chlorin, and "natural" PSs i.e protoporphyrin IX (PpIX) and chlorin e6 (Ce6). The objectives of our research were the synthesis and photophysical characterization of PSs to evaluate the influence of the nature of the PS and the addition of a spacer onto the photophysical properties of the conjugates (Figure 1).

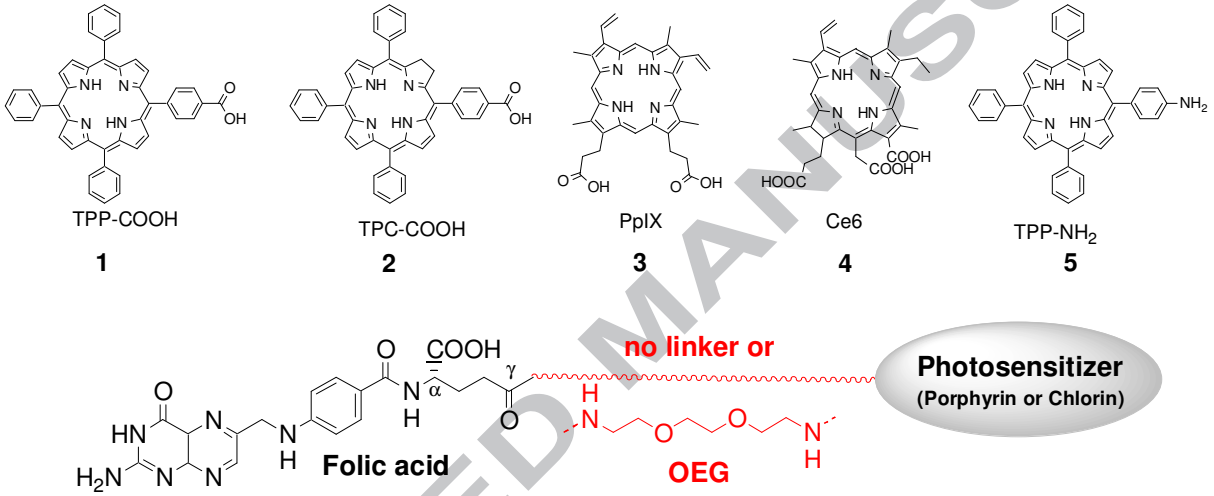

Figure 1. Folic acid conjugate

2. Chemistry

1.1. Synthesis

Our strategy for the synthesis of PS-FA conjugates **12**-**13** was divided into three main parts and is shown in Scheme 1: first, the preparation of tetraphenylporphyrin monocarboxylic acid TPP-COOH (**1**) and tetraphenylchlorin monocarboxylic acid TPC-COOH **2**, second the addition of a small oligo(ethylene glycol), 2,2'-(ethylenedioxy)-diethylamine abbreviated OEG, third coupling to FA to give the corresponding conjugates.

Tetraphenylchlorin monocarboxylic acid TPC-COOH **2** was synthesized using the Lindsey method[42] to produce first porphyrin TPP-COOH **1** and Whitlock di-imide reduction of this last porphyrin[43] (Scheme 2). Activation of the carboxylic function of the starting porphyrins was performed by esterification of these porphyrins with *N*-hydroxysuccinimide (NHS) in dichloromethane with *N,N'*-dicyclohexylcarbodiimide (DCC) as catalyst. Good yields of TPP-NHS **6** and TPC-NHS **7** were obtained - 75 % and 89 %, respectively.

* Corresponding author: address Email: celine.frochot@univ-lorraine.fr

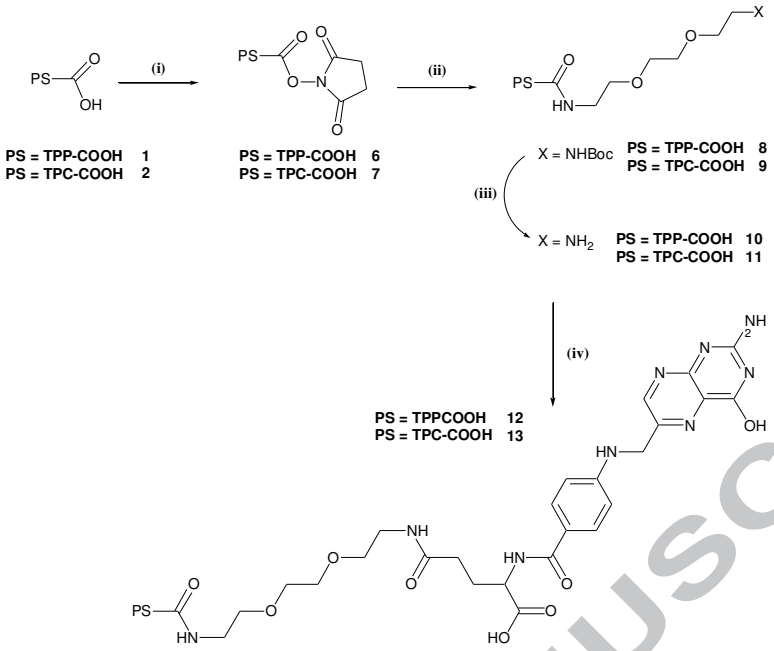

Scheme 1. Synthesis strategy for PS-OEG-FA **12, 13**. (i) NHS, DCC, CH_2Cl_2, 45 °C, overnight. (ii) OEG (*N*-Boc-2,2´-(ethylenedioxy)diethylamine), THF, r.t., 18-24 h. (iii) TFA, r.t., 2h. (iv) FA, DCC, pyridine, DMSO, r.t., 24h

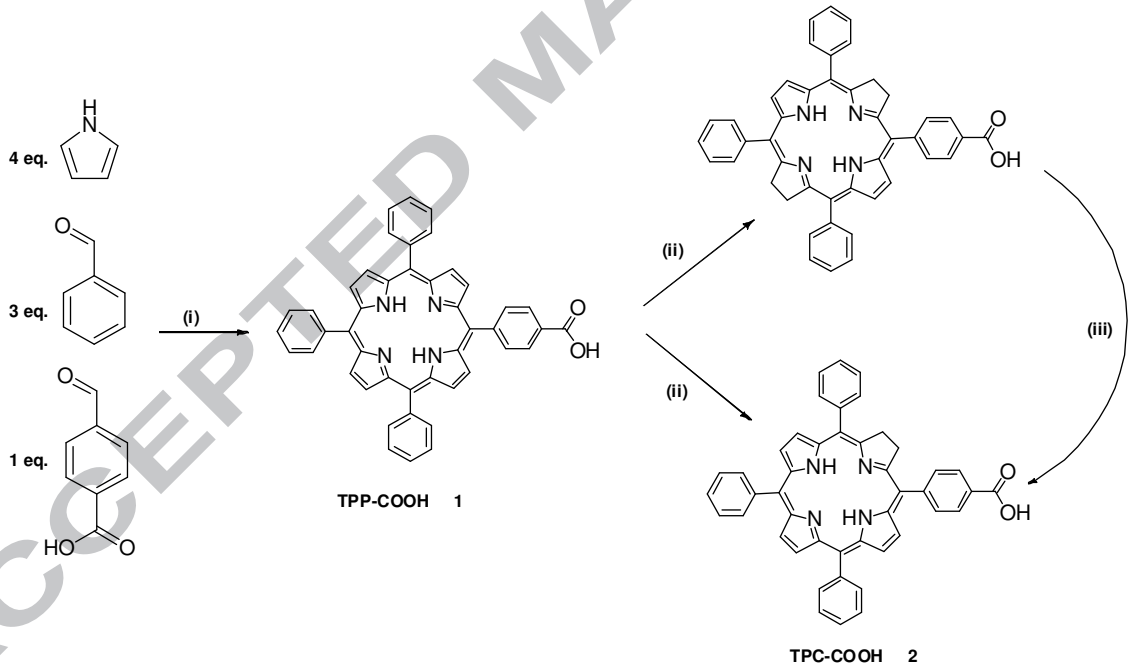

Scheme 2. Synthesis of photosensitizers TPP-COOH **1** and TPC-COOH **2**. (i) $BF_3.(OEt)_2$, CH_2Cl_2, reflux, overnight and then, *p*-chloranil. (ii) *p*-TSH, K_2CO_3, pyridine, reflux, overnight. (iii) EtOAc, *o*-chloranil.

TPP- and TPC-OEG-NHBoc **8** and **9** were synthesized from TPP- and TPC-NHS **6** and **7** with *N*-Boc-2,2´-(ethylenedioxy)diethylamine in THF at room temperature as previously described[17]. Yields were comprised between 70% and 80 %. For the purification of compounds **8** and **9** on silica gel columns, CH_2Cl_2/EtOH (or MeOH) was preferred to acetone/CH_2Cl_2/hexane (at a ratio of 1:4:5) as we previously described[17] for similar compounds. A better separation of side-products could be observed without using hexane. The Boc group was removed by using trifluoroacetic acid (TFA) to give the amine photosensitizers **10** and **11**. Finally, these amine porphyrins were coupled to DCC-activated FA in pyridine/DMSO to give the conjugates **12** and **13** after purification by RP-HPLC.

To evaluate the influence of the nature and distance of the PS from FA on the photophysical properties, we synthesized a porphyrin directly coupled to FA (Scheme 3). The 5-(4-aminophenyl)-10,15,20-triphenylporphyrin (TPP-NH_2 **5**) was coupled to FA activated by DCC in pyridine/DMSO to give the conjugate **14** at 4 % yield after purification by RP-HPLC. This rather poor yield can be attributed to the very low reactivity of the amine of the compound **5** and also to an inadequate choice of the coupling reagent. Activation of this amine by isothiocyanate (NCS) may help to ameliorate the coupling of the TPP-NH_2 **5** with folic acid.

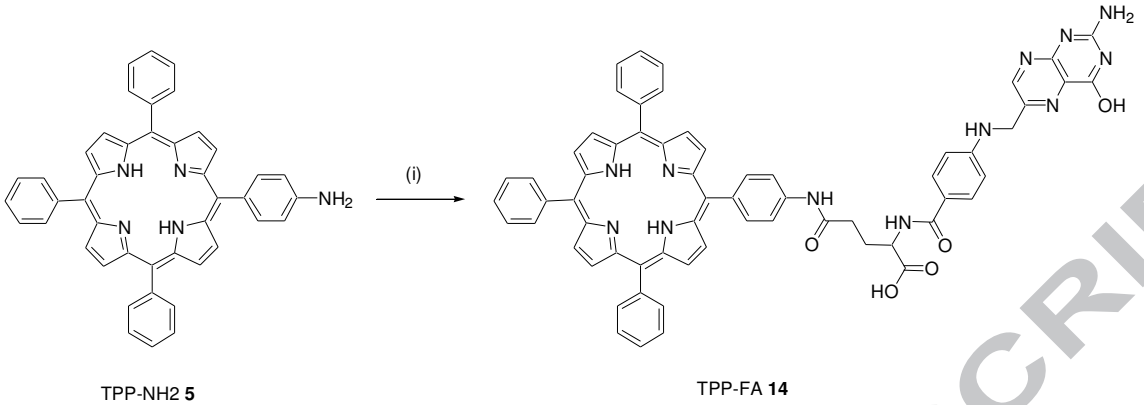

Scheme 3. Synthesis of TTP-FA **14**: (i) FA, DCC, pyridine, DMSO, r.t., 48h.

Secondly, we shall report on our synthesis of "natural" photosensitizer-FA conjugates **19** and **20**. As "natural" porphyrin moieties, we used either PpIX **3** or Ce6 **4**, which are the most well-known natural PSs possessing carboxylic functions used *in vivo* for clinical applications.

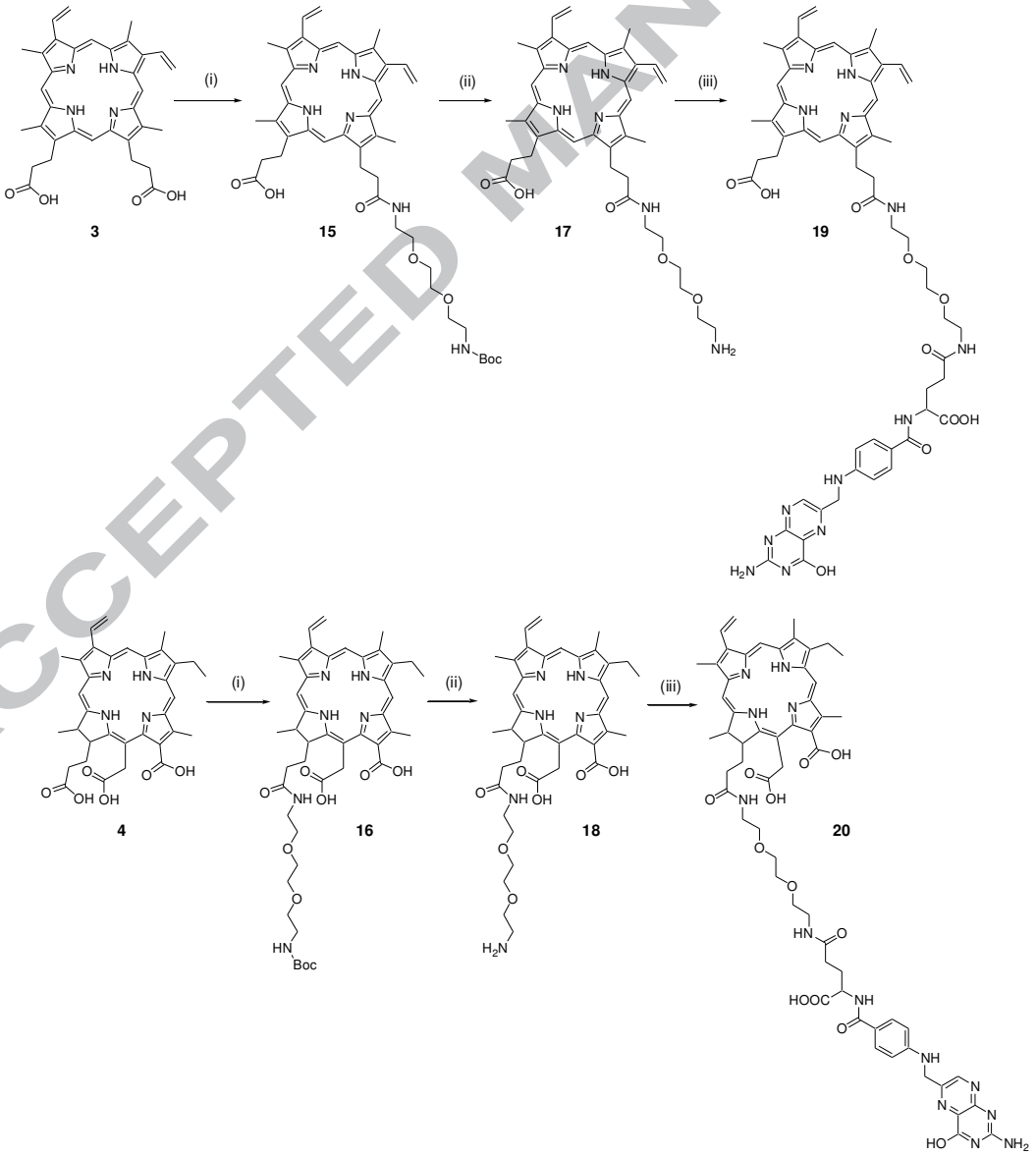

Scheme 4. Syntheses of PpIX- OEG-FA **19** and Ce6- OEG-FA **20**: (i) Spacer (*N*-Boc-2,2´-(ethylenedioxy)diethylamine), DCC, HOBt, DMF, r.t., 24h. (ii) TFA, r.t., 2h. (iii) FA, DCC, pyridine, DMSO, r.t., 24h.

Protoporphyrin IX **3** or chlorin e6 **4** (Scheme 4) reacted with *N*-Boc-2,2´-(ethylenedioxy)diethylamine in DMF in by adding dicyclohexylcarbodiimide (DCC) and 1-hydroxybenzotriazole (HOBt). After purification through a silica gel column (eluent: CH_2Cl_2/EtOH gradient 100:0 to 0:100 +1% Et_3N), mono-protected OEG protoporphyrin IX **15** and mono-protected OEG chlorin e6 conjugates **16** were obtained at 43% and 39% yields, respectively. The Boc group was removed by TFA and the expected conjugates **19** and **20** were obtained at 53% and 45% yields respectively, by coupling with FA which was activated by DCC in pyridine/DMSO after precipitation in cold diethyl ether followed by centrifugation.

All the yields are reported in Table 1.

Considering only the "synthesis" parameter, even if the coupling of FA to TPP-NH_2 was merely one step, the best yield was obtained for the two natural commercial PSs Ce6 and PpIX.

Table 1. Yield of all the steps, overall yield and number of steps for each compound

	Commercial or synthesized	PS-NHS	PS-OEG-Boc	PS-OEG-NH_2	PS- OEG-FA	Overall	Nb of steps
TPP-COOH	11	75	73	85	28	1.4	5
TPC-COOH	7	89	78	24	62	1	6
PpIX	-	-	43	49	53	11.2	3
Ce6	-	-	39	52	45	9.1	3
TPP-NH_2	-	-	-	-	4	4	1

1.2. Hydrophobicity of molecules

To compare the hydrophobicity of PSs alone and that of the corresponding PSs after coupling with FA (PS-OEG-FA), we looked at the retention time of each molecule in reverse phase HPLC on a C_{18} column using an acetonitrile/water gradient (10/90 % to 100/0 % in 25 min, 100/0% for 15 min, acetonitrile/water, v/v). The comparison of retention times and consequently hydrophobicities are shown in figure 2. A long retention time indicates a high hydrophobicity and vice versa. As expected, the more carboxylic functions presented by the compounds, the less hydrophobic they are. Indeed, the order of hydrophobicity is Ce6 (3 carboxylic functions) < PpIX (2 carboxylic functions) < TPP-NH_2 (1 amine function that might be protonated due to the presence of 0.1 % TFA in the water) < TPP-COOH (1 carboxylic function) < TPC-COOH. When coupled to FA, all the compounds have lower retention times than the same compounds without FA. The coupling of FA to TPP-NH_2 or TPP-OEG leads to compounds with the same retention time. It seems that the introduction of the short OEG unit does not significantly decrease the hydrophobicity of the compound. This is probably due to the small size of the OEG. In a previous study [3], we evaluated the influence of three spacers (aminohexanoic acid (Ahx), 1-amino-3,6-dioxaoctanoic acid (PEG9), and 1-amino-9-aza-3,6,12,15-tetraoxa-10-on-heptadecanoic acid (PEG18)) on the hydrophilicity of (5-(4-carboxyphenyl)-10,15, 20-triphenyl chlorin coupled to DKPPR or TKPRR peptide *via* these spacers. The reverse phase retention times for TPC–Ahx–DKPPR, TPC–PEG9–DKPPR and TPC–PEG18–DKPPR were 19.35, 19.05 and 18.02 min respectively. For TPC–Ahx–TKPRR, TPC– PEG9–TKPRR and TPC– PEG18–TKPRR we found 17.37, 17.31, and 16.94 min. The retention time of the conjugate was inversely proportionated to their polarity. By increasing the length of our spacer, we probably induced a decrease in the polarity of our targeted photosensitizer. If we consider the parameter "hydrophobicity", the best candidates could be Ce6 and PpIX.

Figure 2 shows the comparison of the hydrophobicities of PS and FA-targeted PS. Each FA-targeted PS presents several retention times due to the formation of isomers. Indeed, carbodiimide-activated FA can link to either α-or γ-carboxyl groups of the glutamate residue. For example, TPC possesses two isomers and then TPC-OEG-FA possesses four due to the coupling of each TPC isomer to α- or γ–carboxyl groups of FA. By RP-HPLC, we determined that around 70% of the PSs were linked through the γ-carboxyl group. This is important information since only the γ-conjugate can bind to FR.

new figure

Figure 2. Comparison of the hydrophobicities of PS and FA-targeted PS (reverse phase HPLC (C18 column), acetonitrile/water gradient (10/90 % à 100/0 % in 25 min, 100/0% for 15 min, acetonitrile/water, v/v)). UV-Detection at 415 nm.

1.3. Photophysical properties

We recorded the absorption and fluorescence spectra of all the photosensitizers in DMSO. DMSO was chosen because it was the only solvent in which all the photosensitizers were totally soluble. In figures 3 and 4, the absorption and fluorescence spectra of the non-targeted and FA-targeted photosensitizers are included.

new figure

Figure 3. (a) Absorption spectra of photosensitizers in DMSO; (b) Absorption spectra of FA-targeted photosensitizers in DMSO at the same concentration (C= 4.9 E^{-6} M)

new figure

Figure 4. (a) Fluorescence spectra of photosensitizers in DMSO; (b) Fluorescence spectra of FA-targeted photosensitizers in DMSO at the same DO.

The photophysical properties of PSs do not change drastically after coupling with FA as seen in Table 2 where we reported epsilons, fluorescence and singlet oxygen quantum yields and lifetimes.

The introduction of FA can lead to changes in the photophysical properties which are different for the various compounds. Nevertheless, all of the FA targeted-PSs were still found to produce fluorescence and $^1O_2$. For Ce6 a decrease of Φ_f and $\Phi\Delta$ can be observed. For TPC-COOH, $\Phi\Delta$ decreases whereas Φ_f is not modified. For TPP-COOH and PpIX Φ_f were found to decrease whereas increased. It was found that TPP-FA is a good fluorescent probe and a good singlet oxygen photosensitizer while TPP-NH_2 is much less efficient.This phenomena might be due to the quenching of the singlet excited state by the amino moietie due to a photoinduced electron transfer as suggested by Jiang et al.[44]

Table 2. Photophysical properties of FA-targeted photosensitizers in DMSO.

Compound	ε ($L.mol^{-1}.cm^{-1}$)							λ_{exc} (nm)	Φ_f (%)	Φ_Δ (%)	τ_f (ns)	τ_Δ(µs)
	Soret Band (λ_{max})	Soret Band (420 nm)	Q_{IV}	Q_{III}	Q_{II}	Q_I	285 nm					
TPP-COOH	411224 (418 nm)	391 429	17 347	8367	5510	4 898	13061	414	15	39	11.5	8.3
TPP-OEG-FA	231224 (419 nm)	223 673	7755	2653	1020	1429	31837	414	9	51	11.4	6
TPC-COOH	77347 (420 nm)	77 347	4898	3469	1429	9796	4082	414	44	51	10.3	11.6
dTPC-OEG-FA	120816 (420 nm)	120 816	6735	5918	3265	21224	53877	414	46	24	11.1	10.1
PpIX	165510 (406 nm)	93 469	15918	12857	8367	6122	12041	414	9	27	15.1	6.8
PpIX-OEG-FA	76531 (407 nm)	47 347	5714	4286	2449	1224	37551	414	8	43	12.6	6.9
Ce6	113218 (405 nm)	45 542	10759	5701	4761	35773	14732	414	31	53	5.9	7.1
Ce6-OEG-FA	119739 (406 nm)	53 796	8736	2299	1954	35251	39427	414	15	31	4.7	8.2
TPP-NH_2	266531 (419 nm)	263 673	16939	12449	7347	6939	17959	414	1	0	1.3	0
TPP-FA	351429 (420 nm)	351 429	15918	9184	5510	5306	44490	414	10	63	11	6.4

Photodynamic dose is proportional to [PS]*(j*t)*[$^3O_2$]*ε*Φ_Δ where [PS] is the PS concentration, (j*t) is the light fluence, [$^3O_2$] = the concentration of O_2 in the medium, ε = the molar extinction coefficient and Φ_Δ the singlet oxygen quantum yield. In the case of PDT treatment, it should be possible to keep (j*t), [$^3O_2$] and [PS] constant for all compounds. The efficiency will be due to ε and Φ_Δ.

In figure 5, we have described the Epsilon of QI, fluorescence quantum yield and singlet oxygen quantum yield of the FA-targeted PSs in DMSO to determine which FA-targeted PS would be the best for PDT applications, that is to say which PS

presents the best epsilon and singlet oxygen quantum yield, as well as a modest fluorescence quantum yield enabling the detection of the compound.

new figure

Figure 5. Epsilon of QI, fluorescence quantum yield and singlet oxygen quantum yield of the FA-targeted photosensitizers in DMSO.

If we consider the parameters Φ_Δ and epsilon at QI, Ce6 seems the best compound. Nevertheless, in clinical practice for porphyrin and chlorin, two lasers sources are mainly used, 635 nm for PpIX and 652 nm for the chlorin Foscan. In table 3, we report ε (635 nm)* Φ_Δ and ε (635 nm)* Φ_Δ for all the FA-targeted photosensitizers.

Table 3. ε (635 nm)*Φ_Δ and ε (652 nm)*Φ_Δ for all the FA-targeted photosensitizers.

compound	ε (635 nm)	ε (652 nm)		ε (635 nm)*	ε (652 nm)*
TPP-FA	2653	408	0.63	1671	257
TPP-OEG-FA	612	204	0.51	312	104
TPC-OEG-FA	2245	21224	0.24	539	5094
Ce6-OEG-FA	204	14286	0.31	63	4429
PpIX-OEG-FA	408	204	0.43	175	88

Clearly for an excitation at 635 nm, TPP-FA is the PS that absorbs the most. For an excitation at 652 nm, TPC-OEG-FA and Ce6-OEG-FA present the highest ε (652 nm)*Φ_Δ. Moreover, these two compounds are the most hydrophilic.

Finally, if we take into account the water solubility and all the photophysical parameters, Ce6-OEG-FA appears to be the best candidate. This is not surprising and was indeed submitted by K.S. Park in a patent in 2014[35]. However the synthesis of this compound is not a trivial matter because of its three free carboxylic functions. Some isomers can be formed during synthesis and purification of the required isomer can be time-consuming.

2. Conclusion

We synthesized 5 FA-targeted photosensitizers. We choose two different classes of photosensitizers - "synthetic" photosensitizers i.e. a porphyrin, a chlorin, and "natural" photosensitizers i.e PpIX and Ce6. An OEG spacer was added between the FA and the photosensitizer except for one compound (a porphyrin directly linked to FA). We can conclude that for these photosensitizers, the introduction of an OEG does not significantly improve the hydrophilicity of the FA-porphyrin. Moreover, all the FA-targeted photosensitizers present good to very good photophysical properties. The best one appears to be Ce6 even if this compound might be difficult to synthesize in large quantities and with a high level of purity due to its chemical structure. In order to evaluate the influence on the photosensitizers onto affinity for FA receptor, we plan to perform affinity experiments *in vitro* on cells expressing RAF (KB) and cells that do not express RAF as well as competition assays. For the best candidate, *in vivo* tests will be also performed.

3. Experimental section

3.1. Chemicals

Chlorin e6 (Ce6 **4**) was purchased from Frontier Scientific. 5-(4-aminophenyl)-10,15,20-triphenylporphyrin (TPP-NH_2 **5**) was purchased from Porphychem. Protoporphyrin IX (PpIX **3**), *N*-Boc-2,2´-(ethylenedioxy)diethylamine ($MW_{OEG\text{-}Boc}$ = 248.32 g/mol) and all other chemicals were obtained from Sigma-Aldrich. Reverse-phase high-performance liquid chromatography (HPLC) was performed on Prostar HPLC (Varian). Analytical HPLC were done with a Pursuit 5-C_{18} column (2.5 µm, 4.6 × 150 mm, Varian) and preparative HPLC with Pursuit 5-C_{18} column (5 µm, 21.2 × 150 mm, Varian), both using a photodiode array detector (UV-Visible detection, Varian) and a fluorescence detector (Varian). NMR spectra (^{1}H, COSY and TOCSY) were recorded on a BRUKER AVANCE spectrometer at 300 MHz. Mass spectra were recorded on LCMS-2010 EV of Shimazu. High resolution mass spectrometry (HRMS) experiments were performed on a micro-Tof Bruker (electrospray ionization ESI +, 50-1000 in low and 50-2500 in width).

Absorption spectra were recorded on a UV-3600 UV-visible double beam spectrophotometer (SHIMADZU, MARNE LA VALLEE, France). Fluorescence spectra were recorded on a Fluorolog FL3-222 spectrofluorimeter (HORIBA Jobin Yvon, LONGJUMEAU, France) equipped with 450 W Xenon lamp, a thermo-stated cell compartment (25°C), a UV-visible photomultiplier R928 (HAMAMATSU Japon) and an InGaAs infrared detector (DSS-16A020L Electro-Optical System Inc, Phoenixville, PA, USA).

Excitation beam is diffracted by a double ruled grating SPEX monochromator (1200 grooves/mm blazed at 330 nm). Emission beam is diffracted by a double ruled grating SPEX monochromator (1200 grooves/mm blazed at 500 nm). Singlet oxygen emission was detected through a double ruled grating SPEX monochromator (600 grooves/mm blazed at 1 µm) and a long-wave pass (780 nm). All spectra were measured in 4 faces quartz cuves. All the emission spectra (fluorescence and singlet oxygen luminescence) have been displayed with the same absorbance (less than 0.2) with the lamp and photomultiplier correction.
Time-resolved experiments were performed using for excitation: a pulsed laser diode emitting at 407 nm (LDH-P-C-400M, FWHM < 70 ps, 1 MHz) coupled with a driver PDL 800-D (both PicoQuant GmbH, BERLIN, Germany) and for detection: an avalanche photodiode SPCM-AQR-15 (EG & G, VAUDREUIL, Canada) coupled with a 650 nm long-wave pass filter as detection system. The acquisition was performed by a PicoHarp 300 module with a 4 channels router PHR-800 (both PicoQuant GmbH, BERLIN, Germany). The fluorescence decays were recorded using the single photon counting method. Data were collected up to 1000 counts accumulated in the maximum channel and analyzed using Time Correlated Single Photon Counting (TCSPC) software Fluofit (PicoQuant GmbH, BERLIN, Germany) based on iterative reconvolution using a Levensberg-Marquandt algoritm, enabling the obtention of multi-exponential profiles (mainly one or two exponentials in our cases).
Singlet oxygen lifetime measurements have be performed on a TEMPRO-01 spectrophotometer (HORIBA Jobin Yvon, LONGJUMEAU, France) composed with a pulsed diode excitation source SpectraLED-415 emitting at 415 nm, a cell compartment, a Seya-Namioka type emission monochromator (600 – 2000 nm) and a H10330-45 near-infrared photomultiplier tube with thermoelectric cooler (HAMAMATSU, Japan) as detection system. The system was monitored by a single photon counting controller FluoroHub-B and the software DataStation and DAS6 (HORIBA Jobin Yvon).

3.2. Synthesis of Photosensitizers

3.2.1. Synthesis of 5-(4-carboxyphenyl)–10,15,20–triphenylporphyrin (TPP-COOH) ***1***

3.5 mL of freshly distilled pyrrole (50 mmol), 3.8 mL of benzaldehyde (37.5 mmol) and 4-carboxybenzaldehyde (1.875 g, 12.5 mmol) were poured into degassed CH_2Cl_2 (700 mL). After 15 min, 0.615 mL of boron trifluoride diethyl ether (5 mmol) was added and the reaction was stirred for 2 hours. Then, p-chloranil (9.225 g, 37.5 mmol) was introduced. The mixture was stirred at 60 °C overnight in the dark, under nitrogen. The solvent was removed. Column chromatography on silica gel (CH_2Cl_2/EtOH, 97/3, v/v) was achieved to purify the crude product, yielding compound 1 (738.5 mg, 11%) as purple crystals. Rf = 0.35 (CH_2Cl_2/EtOH = 97:3, v/v). ^{1}H NMR (300 MHz, DMSO-d_6): δ (ppm) = -2.92 (s, 2H, $NH_{pyrrole}$), 7.83 (s, 9H, $H_{m\text{- and }p\text{-phenyl}}$), 8.24 (d, 6H, $H_{o\text{-phenyl}}$), 8.37 (dd, 4H, $H_{o\text{-phenyl-COOH}}$), 8.84 (s, 8H, Hβ-pyrrole), 13.24 (br, 1H, COOH). HRMS (ESI+): m/z calculated for $C_{45}H_{30}N_4O_2$ $[M+H]^+$ 659.2442; found 659.2476.

3.2.2. Synthesis of 5-(4-carboxyphenyl)-10,15,20-triphenylchlorin (TPC-COOH) ***2***

The synthesis was performed according to the protocol described by Laville et al.[45]: **1** (200 mg, 0.30 mmol), K_2CO_3 (1.26 g; 9 mmol) and p-toluenesulfonylhydrazide (1.70 g, 9 mmol) were dissolved in freshly distilled pyridine (20 mL) and stirred overnight at pyridine reflux (110 °C) in a round bottom flask isolated from light and under inert atmosphere. After cooling, ethyl acetate (50 mL) and water (50 mL) were added and the solution was heated at 100 °C for 1 hour. The organic phase was separated and washed with HCl (1 M, 200 mL), water (500 mL) and a saturated water solution of $NaHCO_3$. By UV–visible spectroscopy we could control the presence or not of chlorin and bacteriochlorin (bands at 650 and 735 nm, respectively). Then the organic phase was concentrated and lyophilized. The dark red solid obtained was dissolved in ethyl acetate (50 mL). Additions of 100 µL of *o*-chloranil (*o*-chloranil solution 300 mg/mL in EtOAc) were poured every 30 min into solution under stirring at room temperature until the disappearance of the 735 nm-bacteriochlorin absorption peak. 100 mL of water was added to quench the reaction (*o*-chloranil in excess). The solution was washed with an aqueous solution of $NaHSO_3$ (5%, 200 mL) in 500 mL water and the organic phase was concentrated. The crude product was purified by HPLC using a MeOH/water (0.1% TFA) [75:25] to MeOH 100% gradient in 30 min, followed by 15 min of isocratic MeOH. R_t = 15.6 and 16.6 min. Yield in **2** (169.9 mg, 61%). ^{1}HNMR (300 MHz, DMSO-d_6): δ (ppm) = -1.59, -1.52 (2 x s, 2H, $NH_{pyrrole}$), 4.13 (s, 4H, CH_2), 7.74 (s, 9H, $H_{m\text{- and }p\text{-phenyl}}$), 7.91, 8.06 (2 x d, 2H + 4H, $H_{o\text{-phenyl}}$), 8.18 (dd, 4H, $H_{o\text{-phenyl-COOH}}$), 8.30 (s, 4H, $H_{\beta\text{-pyrrole}}$), 8.59 (s, 2H, $H_{\beta\text{-pyrrole}}$). HRMS (ESI+): m/z calcd. for $C_{45}H_{32}N_4O_2$ $[M+H]^+$ 661.2598; found 661.2636.

3.3. Synthesis of succinimide ester Photosensitizers ***6, 7***

In the dark and under an inert atmosphere, the corresponding PS-COOH (1 eq.) was dissolved in CH_2Cl_2 (20-50 mL) and *N*-hydroxysuccinimide (3 eq.) and *N,N'*-dicyclohexylcarbodiimide (3 eq.) were added. The mixture was stirred at 40 °C, for 4 hours, under argon.

3.3.1. Synthesis of 5-(4-carboxyphenylsuccinimide ester)–10,15,20–triphenylporphyrin (TPP-NHS) ***6***

Purification of the crude material was performed using a silica gel column with CH_2Cl_2. Compound **6** was obtained after recrystallization in CH_2Cl_2/hexane, as a purple solid at a yield of 75% (377.3 mg). R_f = 0.79 (CH_2Cl_2/EtOH = 97/3, v/v). ^{1}H NMR (300 MHz, DMSO-d_6): δ (ppm) = -2.91 (s, 2H, $NH_{pyrrole}$), 3.00 (s, 4H, CH_2), 7.84 (s, 9H, $H_{m\text{- and }p\text{-phenyl}}$), 8.22 (d, 6H, $H_{o\text{-phenyl}}$), 8.50 (dd, 4H, $_{o\text{-phenyl-COOH}}$),), 8.85 (s, 8H, $H_{\beta\text{-pyrrole}}$). HRMS (ESI+): m/z calcd. for $C_{49}H_{33}N_5O_4$ $[M+H]^+$ 756.2605; found 756.2588.

3.3.2. Synthesis of 5-(4-carboxyphenylsuccinimide ester)-10,15,20-triphenylchlorin (TPC-NHS) ***7***

Purification of the crude material was performed using a silica gel column with CH_2Cl_2. Compound **7** was obtained, after recrystallization in CH_2Cl_2/hexane, as a purple solid with a yield of 89% (102.6 mg). R_f = 0.17 (CH_2Cl_2 = 100 %). ^{1}HNMR (300 MHz, DMSO-d_6): δ (ppm) = -1.61, -1.48 (2 x s, 2H, $NH_{pyrrole}$), 2.98 (s, 4H, NHS-CH_2), 4.13 (s, 4H, CH_2), 7.74 (s, 9H, $H_{m\text{- and }p\text{-phenyl}}$), 7.90, 8.08(2 x d, 2H + 4H, $H_{o\text{-phenyl}}$), 8.19 (dd, 4H, $H_{o\text{-phenyl-COOH}}$), 8.32 (s, 4H, $H_{\beta\text{-pyrrole}}$), 8.42 (s, 2H, $H_{\beta\text{-pyrrole}}$). HRMS (ESI+): m/z calcd. for $C_{49}H_{35}N_5O_4$ $[M+H]^+$ 758.2762; found 758.2796.

Following procedures were adapted from previous protocols.*[27, 46]*

*3.4. Synthesis of Photosensitizer-OEG-NHBoc derivatives **8, 9, 15** and **16***

*3.4.1. Synthesis of TPP-OEG-NHBoc **8***

84 mg of compound **6** (0.11 mmol) and 26.3 mg of *N*-Boc-2,2´-(ethylenedioxy)diethylamine (0.11 mmol) were dissolved in 30 mL of THF. The reaction mixture was stirred at room temperature, under a nitrogen atmosphere in the dark for 18 hours. The solvent was removed by vacuum. Silica gel column with 3% EtOH in CH_2Cl_2 was used to purify the crude material and compound **8** was obtained as a purple solid with a yield of 73% (68.7 mg). R_f = 0.32 (CH_2Cl_2/EtOH = 97/3, v/v). ^{1}H NMR (300 MHz, DMSO-d_6): δ (ppm) = -2.92 (s, 2H, $NH_{pyrrole}$), 1.35 (s, 9H, Boc), 3.11 (q, 2H, $CH_{2\ OEG}$), 3.45 (q, 2H, $CH_{2\ OEG}$), 3.60 (m, 8H, $CH_{2\ OEG}$), 7.81 (s, 9H, $H_{m\text{- and }p\text{-phenyl}}$), 8.22 (d + s, 10H, $H_{o\text{-phenyl-COOH}}$ and $H_{o\text{-phenyl}}$), 8.83 (s, 8H, $H_{\beta\text{-pyrrole}}$). HRMS (ESI+): m/z calcd. for $C_{56}H_{52}N_6O_5$ $[M+H]^+$ 889.4072; found 889.4059.

*3.4.2. Synthesis of TPC-OEG-NHBoc **9***

114 mg of compound **7** (0.15 mmol) and 37.6 mg of *N*-Boc-2,2´-(ethylenedioxy)diethylamine (0.15 mmol) were dissolved in 30 mL of THF. The reaction mixture was stirred at room temperature under nitrogen in the dark for 24 hours. The solvent was removed under vacuum. Silica gel column with 3% EtOH in CH_2Cl_2 was used to purify the crude material and compound **9** was obtained as a purple solid with a yield of 78% (105.3 mg). R_f = 0.34 (CH_2Cl_2/EtOH = 97/3, v/v). ^{1}H NMR (300 MHz, DMSO-d_6): δ (ppm) = -1.58, -1.53 (2 x s, 2H, $NH_{pyrrole}$), 1.35 (s, 9H, Boc), 3.09 (q, 2H, $CH_{2\ OEG}$), 3.42 (q, 2H, $CH_{2\ OEG}$), 3.61 (m, 8H, $CH_{2\ OEG}$), 4.13 (s, 4H, CH_2), 7.73 (s, 9H, $H_{m\text{- and }p\text{-phenyl}}$), 7.92, 8.06 (2 x d, 2H + 4H, $H_{o\text{-phenyl}}$), 8.10 (dd, 4H, $H_{o\text{-phenyl-COOH}}$), 8.27 (s, 4H, $H_{\beta\text{-pyrrole}}$), 8.57 (s, 2H, $H_{\beta\text{-pyrrole}}$). HRMS (ESI+): m/z calcd. for $C_{56}H_{54}N_6O_5$ $[M+H]^+$ 891.4228; found 891.4214.

*3.4.3. Synthesis of PpIX-OEG-NHBoc **15***

N-Boc-2,2´-(ethylenedioxy)diethylamine (1.1 eq.) was dissolved in 2 mL of DMF. Protoporphyrin IX (100 mg) and *N,N*-dicyclohexylcarbodiimide (DCC) (1.1 eq.) dissolved in dry DMF (5 mL) were added. 1-hydroxybenzotriazole (HOBt) (1.1 eq.) was then introduced. The mixture protected from light was stirred for 24 hours under argon. DMF was then evaporated and the crude product was solubilized in CH_2Cl_2. The organic layer was washed with water (2 x 50 mL), dried with $MgSO_4$, and CH_2Cl_2 was evaporated. The pure product **15** was obtained with a yield of 43% after purification with silica gel column. ^{1}H NMR (300 MHz, $CDCl_3$): δ (ppm) = 1.28 (s, 9H, Boc), 1.87 (m, 2H, CH_2), 2.23 (m, 2H, CH_2), 2.48 (m, 2H, CH_2), 2.73 (m, 2H, CH_2), 3.52 - 2.90 (m, 20H, $4CH_{3\beta\ pyrrole}$ + $4CH_{2\ OEG}$), 4.02 (brd, 2H, CH_2), 4.18 (brd, 2H, CH_2), 4.53 (brs, 1H, NHCO), , 6.31 - 6.05 (m, 4H, CH_{2vinyl}), 6.64 (s, 1H, NHBoc), 8.17 – 7.93 (m, 2H, CH_{vinyl}), 9.41, 9.64, 9.80 (s, 4H, H_{meso}). MS (ESI+): m/z calcd. for $C_{45}H_{56}N_6O_7$ $[M+H]^+$ 792.96; found 792.9603.

*3.4.4. Synthesis of Ce6-OEG-NHBoc **16***

N-Boc-2,2´-(ethylenedioxy)diethylamine (1 eq.) was dissolved in 1 mL of DMF. A solution of chlorin e6 **4** (200 mg) and *N,N*-dicyclohexylcarbodiimide (DCC) (1 eq.) in dry THF/DMF (25/2.5 mL) was added. 1-hydroxybenzotriazole (HOBt) (1.1 eq.) was then introduced. The mixture protected from light was stirred for 24 hours under argon. Solvents were evaporated under vacuum. After purification by column chromatography, the pure product **16** was obtained with a yield of 39% (109 mg). ^{1}H NMR (300 MHz, DMSO-d_6): δ (ppm) = -2.65 (s, 1H, $NH_{pyrrole}$), -2.03 (s, 1H, $NH_{pyrrole}$), 1.23 (s, 3H, CH_3), 1.27 (m, 9H, Boc), 1.37 (s, 3H, $CH_{3\beta\ pyrroline}$), 1.69 (m, 8H, CH_2), 2.84 (m, 2H, CH_2), 3.06 (m, 6H, CH_2), 3.43 (s, 3H, $CH_{3\beta\ pyrrole}$), 3.48 (s, 3H, $CH_{3\beta\ pyrrole}$), 3.54 (s, 3H, $CH_{3\beta\ pyrrole}$), 3.82 (brd, 2H, CH_2-CH_3), 4.33 (brs, 1H, $H_{\beta\ pyrroline}$), 4.53 (brd, 1H, $H_{\beta\ pyrroline}$), 5.10 (m, 2H, CH_2-CO), 5.81 (m, 1H, NHCO), 6.15 (d, 1H, CH_{2vinyl}), 6.44 (d, 1H, CH_{2vinyl}), 8.35 (dd, 1H, CH_{vinyl}), 9.13 (s, 1H, H_{meso}), 9.66 (s, 1H, H_{meso}), 9.78 (s, 1H, H_{meso}). MS (ESI+): m/z calcd. for $C_{45}H_{56}N_6O_7$ $[M+H]^+$ 826.96; found 826.9663

*3.5. Synthesis of PS-OEG-NH2 derivatives **10, 11, 17** and **18***

PS-OEG-NHBoc molecules were dissolved in 2 mL of TFA. The mixture protected from light was stirred for 2 hours under argon. Next, TFA was lyophilized. The colored residue was solubilized in CH_2Cl_2 (10 mL), and anhydrous potassium carbonate was added until the color changed from green to red (for TPP-COOH and TPC-COOH) or from blue to green (for Ce6). After filtration, solvent was evaporated.

*3.5.1. Synthesis of TPP-OEG-NH_2 **10***

Silica gel column with CH_2Cl_2/MeOH (from 80:20 to 50:50, v/v) was used to purify the crude compound yielding **10** (75.1 mg, 85%) as a purple solid. R_f = 0.72 (CH_2Cl_2/MeOH = 1/1, v/v). ^{1}H NMR (300 MHz, DMSO-d_6): δ (ppm) = -2.92 (s, 2H, $NH_{pyrrole}$), 3.33 (m, 2H, $CH_{2\ OEG}$), 3.64 (m + d, 10H, $CH_{2\ OEG}$), 7.83 (s, 9H, $H_{m\text{- and }p\text{-phenyl}}$), 8.22 (d + s, 10H, $H_{o\text{-phenyl-COOH}}$ and $H_{o\text{-phenyl}}$), 8.84 (s, 8H, $H_{\beta\text{-pyrrole}}$). HRMS (ESI+): m/z calcd. for $C_{51}H_{44}N_6O_3$ $[M+H]^+$ 789.3548; found 789.3560.

*3.5.2. Synthesis of TPC-OEG-NH_2 **11***

The residue was purified by HPLC on a C_{18} preparative column using a MeOH/water gradient (75/25 % to 100/0 % in 30 min, 100/0% for 15 min, MeOH/water (0.1% TFA), v/v). The fraction R_t = 8.05 and 9.54 min gave the pure product **11** (21.0 mg, 24%). ^{1}H NMR (300 MHz, DMSO-d_6): δ (ppm) = -1.56, -1.51 (2 x s, 2H, $NH_{pyrrole}$), 3.02 (q, 2H, $CH_{2\ OEG}$), 3.58 (q, 2H, $CH_{2\ OEG}$), 3.74 (s, 8H, $CH_{2\ OEG}$), 4.11 (s, 4H, CH_2), 7.70 (s, 9H, $H_{m\text{- and }p\text{-phenyl}}$), 8.00, 8.07 (2 x d, 2H + 4H, $H_{o\text{-phenyl}}$), 8.20 (dd, 4H, $H_{o\text{-phenyl-COOH}}$), 8.32 (s, 4H, $H_{\beta\text{-pyrrole}}$), 8.57 (s, 2H, $H_{\beta\text{-pyrrole}}$). HRMS (ESI+): m/z calcd. for $C_{51}H_{46}N_6O_3$ $[M+2H]^{2+}$ 396.1880; found 396.1889.

*3.5.3. Synthesis of PpIX-OEG-NH_2 **17***

Compound **15** was dissolved in 2 TFA (2mL) and let under stirring for 2 hours under nitrogen and protected by light. Next, TFA was lyophilized. The red residue was solubilized in CH_2Cl_2/EtOH (20 mL), and anhydrous potassium carbonate was added until the color changed. After filtration, solvent was evaporated. HPLC on a C_{18} preparative column with a acetonitrile/water

gradient (10/90 % to 100/0 % in 45 min, 100/0% for 5 min, acetonitrile/water, v/v) was used to purify the residue. The fraction R_t = 21.7 min gave the pure product **17** (25 mg, 49%). ^{1}H NMR (300 MHz, DMSO-d_6): δ (ppm) = 2.67 (brq, 2H, CH_2), 2.79 (m, 4H, CH_2), 2.80 – 3.09 (m, 8H, $CH_{2\ OEG}$), 3.20 (brt, 2H, $CH_{2\ OEG}$), 3.57 (brd, 6H, $CH_{3\ \beta\text{-pyrrole}}$), 3.63 (bt, 6H, $CH_{3\beta\text{-pyrrole}}$), 4.30 (brd, 4H, CH_2), 6.19 (brd, 2H, $CH_{2\ vinyl}$), 6.38 (brd, 2H, CH_{2vinyl}), 7.58 (brs, 2H, NH_2), 7.82 (brt, 1H, NHCO), 8.45 – 8.35 (m, 2H, CH_{vinyl}), 10.11 – 10.03 (m, 4H, H_{meso}). MS (ESI+): m/z calcd. for $C_{45}H_{56}N_6O_7$ $[M+H]^+$ 692.85; found 692.8527

3.5.4. Synthesis of Ce6-OEG-NH$_2$ ***18***

Compound **16** (109 mg) was dissolved in TFA (4 mL) and let under stirring for 2 hours under nitrogen and protected by light. Next, TFA was lyophilized. The crude product was solubilized in $CHCl_3$/EtOH (2/1), and anhydrous potassium carbonate was added until the color changed from purple to green. After filtration, the solvent was evaporated. HPLC with a C_{18} preparative column and an acetonitrile/water gradient (10/90 % to 100/0 % in 45 min, 100/0% for 5 min, acetonitrile/water, v/v) was used to purify the compound. The fraction R_t = 22.7 min gave the pure product **18** (50 mg, 52%). ^{1}H NMR (300 MHz, DMSO-d_6): δ (ppm) = -2.68 (s, 1H, $NH_{pyrrole}$), -2.03 (s, 1H, $NH_{pyrrole}$), 1.23 (s, 3H, CH_3), 1.35 (s, 3H, $CH_{3\beta\ pyrroline}$), 1.68 (m, 8H, CH_2), 2.83 (m, 2H, CH_2), 3.04 (m, 6H, -CH_2), 3.41 (s, 3H, $CH_{3\beta\ pyrrole}$), 3.46 (s, 3H, $CH_{3\beta\ pyrrole}$), 3.52 (s, 3H, $CH_{3\beta\ pyrrole}$), 3.81 (brd, 2H, CH_2), 4.31 (brs, 1H, $H_{\beta\ pyrrole}$), 4.51 (brd, 1H, $H_{\beta\ pyrrole}$), 5.73 (m, 2H, CH_2-CO), 6.13 (d, 1H, CH_{2vinyl}), 6.43 (d, 1H, CH_{2vinyl}), 7.58 (m, 2H, NH_2), 8.01 (brs, 1H, CONH), 8.35 (dd, 1H, CH_{vinyl}), 9.11 (s, 1H, H_{meso}), 9.62 (s, 1H, H_{meso}), 9.77 (s, 1H, H_{meso}). MS (ESI+): m/z calcd. for $C_{40}H_{50}N_6O_7$ $[M+H]^+$ 726.86; found 726.8579

3.6. Synthesis of Photosensitizer-Spacer-FA derivatives ***12, 13, 19*** *and* ***20***

FA (1 eq.) and DCC (1 eq.) were dissolved in anhydrous DMSO (5 mL) and pyridine (2 mL). The mixture was stirred for 15 min protected by light and under a N_2 atmosphere. Compound PS-OEG-NH_2 (0.9 eq.) was then added and the stirring was continued for 24h. The solution was slowly poured into vigorously stirred cold diethyl ether. By centrifugation, the precipitate obtained was collected and washed with diethyl ether. The powder was dried under high vacuum. HPLC on a C_{18} preparative column with an acetonitrile/water gradient (10/90 % to 100/0 % in 25 min, 100/0% for 15 min, acetonitrile/water, v/v) was used to purify the compound.

3.6.1. Synthesis of TPP-OEG-FA ***12***

The fraction R_t = 17.9 and 18.0 min gave the pure product **12** (30 mg, 28%). ^{1}H NMR (300 MHz, DMSO-d_6): δ (ppm) = -2.92 (s, 2H, $NH_{pyrrole}$), 2.07 (m, 2H, $CH_{2\ FA}$), 2.30 (m, 2H, $CH_{2\ FA}$), 3.60 (m, 8H, $CH_{2\ OEG}$), 4.40 (m, 1H, $NH_{\ FA}$), 4.48 (d, 2H, $CH_{2\ FA}$), 6.58 (d, 2H, $H_{arom\ FA}$), 6.88 (m, 3H, NH + NH_2), 7.84 (s, 9H, $H_{m\text{- and }p\text{-phenyl}}$), 8.22 (d, 6H, $H_{o\text{-phenyl}}$), 8.31 (s, 4H, $H_{o\text{-phenyl-COOH}}$), 8.64 (d, 1H, $CH_{arom\ FA}$), 8.84 (s, 8H, $H_{\beta\text{-pyrrole}}$). HRMS (ESI+): *m/z* calcd. for $C_{70}H_{61}N_{13}O_8$ $[M+H]^+$ 1212.4839; found 1212.4790.

3.6.2. Synthesis of TPC-OEG-FA ***13***

No further purification by HPLC was necessary in this case. The fraction R_t = 20.8; 21.0; 21.2 and 21.4 min gave the pure product **13** (21 mg, 62%). ^{1}H NMR (300 MHz, DMSO-d_6): δ (ppm) = -1.59, -1.54 (2 x s, 2H, $NH_{pyrrole}$), 2.00 (m, 2H, $CH_{2\ FA}$), 2.30 (t, 2H, $CH_{2\ FA}$), 3.57 (m, 8H, $CH_{2\ OEG}$), 4.12 (s, 4H, CH_2), 4.3 (m, 1H, NH), 4.47 (d, 2H, $CH_{2\ FA}$), 6.65 (d, 2H, $H_{arom\ FA}$), 6.91 (m, 3H, NH + NH_2), 7.70 (s, 9H, $H_{m\text{- and }p\text{-phenyl}}$), 8.00, 8.07 (2 x d, 2H + 4H, $H_{o\text{-phenyl}}$), 8.11 (d, 1H, NH), 8.20 (dd, 4H, $H_{o\text{-phenyl-COOH}}$), 8.30 (s, 4H, $H_{\beta\text{-pyrrole}}$), 8.59 (s, 2H, $H_{\beta\text{-pyrrole}}$), 8.64 (d, 1H, $CH_{arom\ FA}$), 11.40 (s, 1H, OH). HRMS (ESI+): *m/z* calcd. for $C_{70}H_{63}N_{13}O_8$ $[M+H]^+$1214.4995; found 1214.4968.

3.6.2.1. Synthesis of PpIX-OEG-FA ***19***

In the dark and under a N_2 atmosphere, FA (1 eq.), DCC (1 eq.) and NHS (1 eq.) were dissolved in anhydrous DMSO (2 mL) . The solution was stirred overnight. FA-NHS was added dropwise to compound **17** (1 eq.) dissolved in 1 mL of DMSO and 0.5 mL of pyridine the stirring was continued for 4 days. The solution was slowly poured into vigorously stirred cold diethyl ether. The precipitate was obtained by centrifugation, washed with both diethyl ether and CH_2Cl_2. The purple powder was dried and **19** was obtained with a yield of 53% (20 mg). ^{1}H NMR (300 MHz, DMSO-d_6): δ (ppm) = -3.84 (s, 2H, $NH_{pyrrole}$), 2.08 (m, 2H, $CH_{2\ FA}$), 2.29 (m, 2H, $CH_{2\ FA}$), 2.88 - 3.24 (m, 16H, CH_2 + $CH_{2\ OEG}$), 3.63 (brd, 6H, $CH_{3\beta\ pyrrole}$), 3.75 (brd, 6H, $CH_{3\beta pyrrol}$), 4.34 (brd, 4H, CH_2), 4.48 (m, 3H, CH_2 and $CHCO_{\ FA}$), 6.20 (brd, 2H, CH_{2vinyl}), 6.44 (brd, 2H, CH_{2vinyl}), 6.55 (d, 2H, $H_{arom\ FA}$), 6.86 (m, 3H, NH + NH_2), 7.63 (d, 2H, $H_{arom\ FA}$), 7.82 (brt, 1H, NHCO), 8.11 (m, 1H, NH), 8.54 (m, 3H, CH_{vinyl}, NHCO), 8.64 (s, 1H, $H_{arom\ FA}$), 10.27 – 10.35 (m, 4H, H_{meso}), 11.39 (s, 1H, OH), 12.24 (brs, 2H, COOH). HRMS (ESI+): *m/z* calcd. for $C_{59}H_{65}N_{13}O_{10}$ $[M+H]^+$ 1116.5; found 1116.5004.

3.6.3. Synthesis of Ce6-OEG-FA ***20***

In the dark and under a N_2 atmosphere, FA (1 eq.), DCC (1 eq.) and NHS (1 eq.) were dissolved in anhydrous DMSO (2 mL), the stirring was continued overnight. FA-NHS was added dropwise to compound **18** (1 eq., 30 mg) in 1 mL of DMSO and 0.5 mL of pyridine. The stirring was continued for 5 days. The solution was slowly poured into vigorously stirred cold diethyl ether. The precipitate was obtained by centrifugation, washed with both diethyl ether and CH_2Cl_2. The green powder **20** was dried and obtained with a yield of 45 % (36 mg). ^{1}H NMR (300 MHz, DMSO-d_6): δ (ppm) = -2.12 (s, 1H, $NH_{pyrrole}$), -1.74 (s, 1H, $NH_{pyrrole}$), 1.26 – 1.39 (m, 6H, CH_3 and $CH_{3\beta\ pyrroline}$), 1.76 (m, 2H, CH_2), 2.05 (m, 2H, $CH_{2\ FA}$), 2.35 (m, 2H, $CH_{2\ FA}$), 2.87 - 3.28 (m, 16H, CH_2 and $CH_{2\ OEG}$), 3.54-3.81 (m, 11H, CH_2 and $3CH_{3\beta\ pyrroline}$), 4.48 (m, 4H, CH_2 and $H_{\beta\ pyrroline}$), 5.17 - 5.39 (m, 2H), 6.17 – 6.90 (m, 6H, $CH_{2\ vinyl}$ and 2 $H_{arom\ FA}$), 7.65 – 8.30 (m, 5H), 8.64 (s, 2H), 9.10 (s, 1H, H_{meso}), 9.74(s, 2H, H_{meso}), 11.44 (s, 1H, OH), 12.2 (brs, 2H, COOH). HRMS (ESI+): *m/z* calcd. for $C_{59}H_{67}N_{13}O_2$ $[M+H]^+$ 1150.5010; found 1150.6350.

3.7. Synthesis of direct linked TPP-FA ***14***

In the dark and under a N_2 atmosphere, FA (74 mg; 0.17 mmol) and DCC (34 mg; 0.17 mmol) were dissolved in a mixture anhydrous DMSO/pyridine (5 mL/2 mL). The solution was stirred for 15 min at room temperature. TPP-NH_2 **5** (105 mg; 0.17 mmol) was then added and the stirring was continued for 48h. The solution was slowly poured into vigorously stirred cold

diethyl ether. The precipitate was obtained by centrifugation, washed with diethyl ether, dried under high vacuum and purified by HPLC with a C_{18} preparative column using an acetonitrile/water gradient (10/90 % to 100/0 % in 45 min, 100/0% for 15 min, acetonitrile/water, v/v). The fraction R_t = 27.4 and 28.3 min gave the pure product **14** (7.3 mg, 4%). ^{1}H NMR (300 MHz, DMSO-d_6): -2.90 (s, 2H, $NH_{pyrrole}$), 2.00 (m, 2H, $CH_{2\ FA}$), 2.35 (t, 2H, $CH_{2\ FA}$), 4.53 (m, 3H, NH + CH_2), 6.67 (dd, 2H, H_{arom}), 7.48 (br, 2H, NH_2), 7.65 (d, 2H, CH_{arom}), 7.80 (d, 2H, $CH_{arom.}$), 7.83 (s, 9H, $H_{m\text{- and }p\text{-phenyl}}$), 8.05 (d, 1H, NH), 8.15 (dd, 4H, $H_{o\text{-phenyl-COOH}}$), 8.28 (d, 6H, $H_{o\text{-phenyl}}$), 8.72 (d, 1H, CH_{arom}), 8.84 (s, 8H, $H_{\beta\text{-pyrrole}}$). HRMS (ESI+): *m/z* calcd. for $C_{63}H_{48}N_{12}O_5$ $[M+Na]^+$ 1075.3763; found 1075.3741.

3.8. Photophysical Properties

The protocols for absorption, fluorescence, and lifetime have been already described elsewhere.[47]

The quantum yield of fluorescence is determined thanks to the equation (1):

$$\Phi_f = \Phi_{f0} \cdot \frac{I_f}{I_{f0}} \cdot \frac{DO_0}{DO} \cdot \left(\frac{n}{n_0}\right)^2 \quad (1)$$

where Φ_f and Φ_{f0}, I_f and I_{f0}, DO and DO_0, n and n_0 are the fluorescence quantum yields, the fluorescence intensities, the optical densities at the excitation wavelength and the refraction indices of the sample and of the reference, respectively.[48, 49]

The quantum yield of singlet oxygen production is determined thanks to the equation (2):

$$\Phi_\Delta = \Phi_{\Delta 0} \cdot \frac{I}{I_{\Delta 0}} \cdot \frac{DO_0}{DO} \quad (2)$$

where Φ_Δ and $\Phi_{\Delta 0}$, I_Δ and $I_{\Delta 0}$, DO and DO_0 are the luminescence quantum yields, the luminescence intensities and the optical densities at the excitation wavelength of the sample and of the reference (Rose bengal $\Phi_{\Delta 0}$ = 0.16) respectively.[50]

References and notes

[1] A.S. Sobolev, D.A. Jans, A.A. Rosenkranz, Targeted intracellular delivery of photosensitizers, Progress in Biophysics and Molecular Biology, 73 (2000) 51-90.

[2] D. Bechet, F. Auger, P. Couleaud, E. Marty, L. Ravasi, N. Durieux, C. Bonnet, F. Plenat, C. Frochot, S. Mordon, O. Tillement, R. Vanderesse, F. Lux, P. Perriat, F. Guillemin, M. Barberi-Heyob, Multifunctional ultrasmall nanoplatforms for vascular-targeted interstitial photodynamic therapy of brain tumors guided by real-time MRI, Nanomed. Nanotechnol. Biol. Med., 11 (2015) 657-670.

[3] E.E. Kamarulzaman, A.M. Gazzali, S. Acherar, C. Frochot, M. Barberi-Heyob, C. Boura, P. Chaimbault, E. Sibille, H.A. Wahab, R. Vanderesse, New peptide-conjugated chlorin-type photosensitizer targeting neuropilin-1 for anti-vascular targeted photodynamic therapy, International Journal of Molecular Sciences, 16 (2015) 24059-24080.

[4] H. Mukai, Y. Wada, Y. Watanabe, The synthesis of Cu-64-chelated porphyrin photosensitizers and their tumor-targeting peptide conjugates for the evaluation of target cell uptake and PET image-based pharmacokinetics of targeted photodynamic therapy agents, Ann. Nucl. Med., 27 (2013) 625-639.

[5] J.C. Mazière, P. Morlière, R. Santus, The role of the low-density-lipoprotein receptor pathway in the delivery of lipophilic photosensitizers in the photodynamic therapy of tumors, J. Photochem. Photobiol. B: Biol., 8 (1991) 351-360.

[6] U. Schmidt-Erfurth, H. Diddens, R. Birngruber, T. Hasan, Photodynamic targeting of human retinoblastoma cells using covalent low-density lipoprotein conjugates, Br. J. Cancer, 75 (1997) 54-61.

[7] D. Lafont, Y. Zorlu, H. Savoie, F. Albrieux, V. Ahsen, R.W. Boyle, F. Dumoulin, Monoglycoconjugated phthalocyanines : effect of sugar and linkage on photodynamic activity, Photodiagnosis Photodyn. Ther. , 10 (2013) 252-259.

[8] F. Bryden, A. Maruani, H. Savoie, V. Chudasama, M.E.B. Smith, S. Caddick, R.W. Boyle, Regioselective and stoichiometrically controlled conjugation of photodynamic sensitizers to a HER2 targeting antibody fragment, Bioconj. Chem., 25 (2014) 611-617.

[9] Y.G. Assaraf, C.P. Leamon, J.A. Reddy, The folate receptor as a rational therapeutic target for personalized cancer treatment, Drug Resist. Updat., 17 (2014) 89-95.

[10] J.A. Ledermann, S. Canevari, T. Thigpen, Targeting the folate receptor: diagnostic and therapeutic approaches to personalize cancer treatments, Ann. Oncol., 26 (2015) 2034-2043.

[11] L. Zeng, L. Luo, Y. Pan, S. Luo, G. Lu, A. Wu, In vivo targeted magnetic resonance imaging and visualized photodynamic therapy in deep-tissue cancers using folic acid-functionalized superparamagnetic-upconversion nanocomposites, Nanoscale, 7 (2015) 8946-8954.

[12] H. Azais, N. Betrouni, S. Mordon, P. Collinet, Targeted approaches and innovative illumination solutions: A new era for photodynamic therapy applications in gynecologic oncology ?, Photodiagnosis Photodyn. Ther., DOI : 10.1016/j.pdpdt.2015.07.006. (2015).

[13] P.X. Li, J.H. Mu, H.L. Xiao, D.H. Li, Antitumor effect of photodynamic therapy with a novel targeted photosensitizer on cervical carcinoma, Oncol. Rep., 33 (2015) 125-132.

[14] M. Grossman, B. Born, M. Heyden, D. Tworowski, G.B. Fields, I. Sagi, M. Havenith, Correlated structural kinetics and retarded solvent dynamics at the metalloprotease active site, Nat. Struct. Mol. Biol., 18 (2011) 1102-U1113.

[15] A.R. Hilgenbrink, P.S. Low, Folate receptor-mediated drug targeting: From therapeutics to diagnostics, J. Pharm. Sci., 94 (2005) 2135-2146.
[16] W. Spiller, H. Kliesch, D. Wohrle, S. Hackbarth, B. Roder, G. Schnurpfeil, Singlet oxygen quantum yields of different photosensitizers in polar solvents and micellar solutions, J. Porphyrins Phthalocyanines, 2 (1998) 145-158.
[17] R.L. Schneider, F. Schmitt, C. Frochot, Y. Fort, N. Lourette, F. Guillemin, J.F. Muller, M. Barberi-Heyob, Design, synthesis, and biological evaluation of folic acid targeted tetraphenylporphyrin as novel photosensitizers for selective photodynamic therapy, Biorg. Med. Chem., 13 (2005) 2799-2808.
[18] J. Han, W. Park, S.J. Park, K. Na, Photosensitizer-conjugated hyaluronic acid-shielded polydopamine nanoparticles for targeted photomediated tumor therapy, Acs Applied Materials & Interfaces, 8 (2016) 7739-7747.
[19] J.V. John, C.W. Chung, R.P. Johnson, Y.I. Jeong, K.D. Chung, D.H. Kang, H. Suh, H. Chen, I. Kim, Dual stimuli-responsive vesicular nanospheres fabricated by lipopolymer hybrids for tumor-targeted photodynamic therapy, Biomacromolecules, 17 (2016) 20-31.
[20] F.J. Ai, Q. Ju, X.M. Zhang, X. Chen, F. Wang, G.Y. Zhu, A core-shell-shell nanoplatform upconverting near-infrared light at 808 nm for luminescence imaging and photodynamic therapy of cancer, Scientific Reports, 5 (2015).
[21] I.T. Teng, Y.J. Chang, L.S. Wang, H.Y. Lu, L.C. Wu, C.M. Yang, C.C. Chiu, C.H. Yang, S.L. Hsu, J.A.A. Ho, Phospholipid-functionalized mesoporous silica nanocarriers for selective photodynamic therapy of cancer, Biomaterials, 34 (2013) 7462-7470.
[22] Y.P. Zeng, S.L. Luo, Z.Y. Yang, J.W. Huang, H. Li, C. Liu, W.D. Wang, R. Li, A folic acid conjugated polyethylenimine-modified PEGylated nanographene loaded photosensitizer: photodynamic therapy and toxicity studies in vitro and in vivo, Journal of Materials Chemistry B, 4 (2016) 2190-2198.
[23] F. Moret, D. Scheglmann, E. Reddi, Folate-targeted PEGylated liposomes improve the selectivity of PDT with meta-tetra(hydroxyphenyl)-chlorin (m-THPC), Photochemical & Photobiological Sciences, 12 (2013) 823-834.
[24] M. Broekgaarden, R. van Vught, S. Oliveira, R.C. Roovers, P. Henegouwen, R.J. Pieters, T.M. Van Gulik, E. Breukink, M. Heger, Site-specific conjugation of single domain antibodies to liposomes enhances photosensitizer uptake and photodynamic therapy efficacy, Nanoscale, 8 (2016) 6490-6494.
[25] J.S. Xu, F. Zeng, H. Wu, C.P. Hu, S.Z. Wu, Enhanced photodynamic efficiency achieved via a dual-targeted strategy based on photosensitizer/micelle structure, Biomacromolecules, 15 (2014) 4249-4259.
[26] L.L. Zhao, T.H. Kim, K.M. Huh, H.W. Kim, S.Y. Kim, Self-assembled photosensitizer-conjugated nanoparticles for targeted photodynamic therapy, J. Biomater. Appl., 28 (2013) 434-447.
[27] V. Morosini, T. Bastogne, C. Frochot, R. Schneider, A. Francois, F. Guillemin, M. Barberi-Heyob, Quantum dot-folic acid conjugates as potential photosensitizers in photodynamic therapy of cancer, Photochemical & Photobiological Sciences, 10 (2011) 842-851.
[28] D. Nicholas, C. Fowley, A.P. McHale, S. Kamila, J. Sheng, J. Atchison, J.F. Callan, A folic acid labelled carbon Quantum Dot - Protoporphryin IX conjugate for use in folate receptor targeted Two-Photon excited Photodynamic Therapy, Proc. SPIE, (2015) 9338 doi:9310.1117/9312.2084821.
[29] Y.Y. Ma, H. Ding, H.M. Xiong, Folic acid functionalized ZnO quantum dots for targeted cancer cell imaging, Nanotechnology, 26 (2015) Article 305702.
[30] R.O. Ogbodu, I. Ndhundhuma, A. Karsten, T. Nyokong, Photodynamic therapy effect of zinc monoamino phthalocyanine-folic acid conjugate adsorbed on single walled carbon nanotubes on melanoma cells, Spectrochim. Acta, Pt. A: Mol. Biomol. Spectrosc., 137 (2015) 1120-1125.
[31] J.W. Tian, L. Ding, Q.B. Wang, Y.P. Hu, L. Jia, J.S. Yu, H.X. Ju, Folate receptor-targeted and cathepsin B-activatable nanoprobe for in situ therapeutic Mmonitoring of photosensitive cell death, Anal. Chem., 87 (2015) 3841-3848.
[32] P. Huang, S.J. Wang, X.S. Wang, G.X. Shen, J. Lin, Z. Wang, S.W. Guo, D.X. Cui, M. Yang, X.Y. Chen, Surface functionalization of chemically reduced graphene oxide for targeted photodynamic therapy, Journal of Biomedical Nanotechnology, 11 (2015) 117-125.
[33] W.T. Liu, L.J. Nie, F.L. Li, Z.P. Aguilar, H. Xu, Y.H. Xiong, F. Fu, H.Y. Xu, Folic acid conjugated magnetic iron oxide nanoparticles for nondestructive separation and detection of ovarian cancer cells from whole blood, Biomaterials Science, 4 (2016) 159-166.
[34] M.R. Ke, S.L. Yeung, D.K.P. Ng, W.P. Fong, P.C. Lo, Preparation and in vitro photodynamic activities of folate-conjugated distyryl boron dipyrromethene based photosensitizers, J. Med. Chem., 56 (2013) 8475-8483.
[35] K.S. Park, E.H. Lee, H.J. Kim, New chlorine e6-folic acid conjugated compound, preparation method thereof, and pharmaceutical composition containing the same for treatment of cancer, 2014.
[36] D.H. Li, P.X. Li, Z.L. Jiang, L.F. Guo, Enhanced tumor targeting and photocytotoxicity of folate-poly(ethylene glycol)-chlorin photosensitizer mediated by folate receptor, Chem. Lett., 42 (2013) 130-131.
[37] C.L. Zhang, C. Li, Y.L. Liu, J.P. Zhang, C.C. Bao, S.J. Liang, Q. Wang, Y. Yang, H.L. Fu, K. Wang, D.X. Cui, Gold nanoclusters-based nanoprobes for simultaneous fluorescence imaging and targeted photodynamic therapy with superior penetration and retention behavior in tumors, Adv. Funct. Mater., 25 (2015) 1314-1325.
[38] K. Stefflova, H. Li, J. Chen, G. Zheng, Peptide-based pharmacomodulation of a cancer-targeted optical imaging and photodynamic therapy agent, Bioconj. Chem., 18 (2007) 379-388.
[39] S. Wang, J. Wang, J.-Y. Chen, Conjugates of folic acids with zinc aminophthalocyanine for cancer cell targeting and photodynamic therapy by one-photon and two-photon excitations, Journal of Materials Chemistry B, 2 (2014) 1594-1602.
[40] Y.W. Zheng, S.F. Chen, B.Y. Zheng, M.R. Ke, J.D. Huang, A silicon(IV) phthalocyanine-folate conjugate as an efficient photosensitizer, Chem. Lett., 43 (2014) 1701-1703.

[41] A. Stallivieri, F. Baros, G. Jetpisbayeva, B. Myrzakhmetov, C. Frochot, The interest of folic acid in targeted photodynamic therapy, Curr. Med. Chem., 22 (2015) 3185-3207.
[42] J.S. Lindsey, S. Prathapan, T.E. Johnson, R.W. Wagner, Porphyrin building-blocks for modular construction of bioorganic model systems, Tetrahedron, 50 (1994) 8941-8968.
[43] H.W. Whitlock Jr, R. Hanauer, M.Y. Oester, B.K. Bower, Diimide reduction of porphyrins, J. Am. Chem. Soc., 91 (1969) 7485-7489.
[44] X.J. Xiong-Jie Jiang, P.C. Lo, S.L. Yeung, W.P. Fong, N. D.K.P,
A pH-responsive fluorescence probe and photosensitiser based on a tetraamino silicon(IV) phthalocyanine, Chem. Commun., 46 (2010) 3188-3190.
[45] I. Laville, T. Figueiredo, B. Loock, S. Pigaglio, P. Maillard, D.S. Grierson, D. Carrez, A. Croisy, J. Blais, Synthesis, cellular internalization and photodynamic activity of glucoconjugated derivatives of tri and tetra(meta-hydroxyphenyl)chlorins, Biorg. Med. Chem., 11 (2003) 1643-1652.
[46] T.H. Tran, B.C. Bae, Y.K. Lee, K. Na, K.M. Huh, Heparin-folate-retinoic acid bioconjugates for targeted delivery of hydrophobic photosensitizers, Carbohydr. Polym., 92 (2013) 1615-1624.
[47] D. Topkaya, P. Arnoux, F. Dumoulin, Modulation of singlet oxygen generation and amphiphilic properties of trihydroxylated monohalogenated porphyrins, J. Porphyrins Phthalocyanines, 19 (2015) 1081-1087.
[48] J.R. Albani, Principles and Applications of Fluorescence Spectroscopy, Principles and applications of fluorescence spectroscopy2007, pp. 1-255.
[49] A.M. Brouwer, Standards for photoluminescence quantum yield measurements in solution (IUPAC Technical Report), Pure Appl. Chem., 83 (2011) 2213-2228.
[50] R.W. Redmond, J.N. Gamlin, A compilation of singlet oxygen yields from biologically relevant molecules, Photochem. Photobiol., 70 (1999) 391-475.

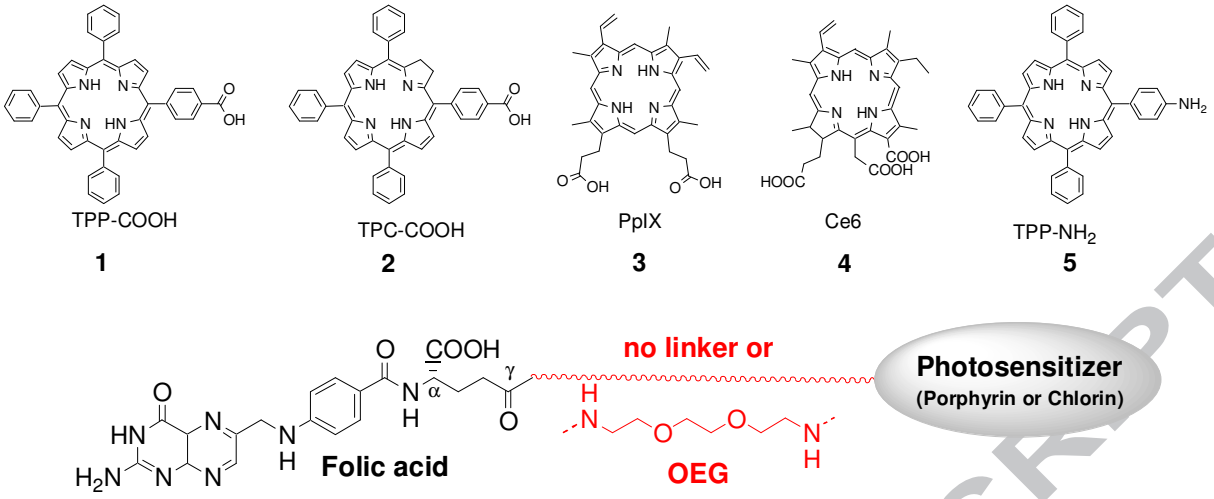

Figure 1. Carrier linked folic acid conjugate system.

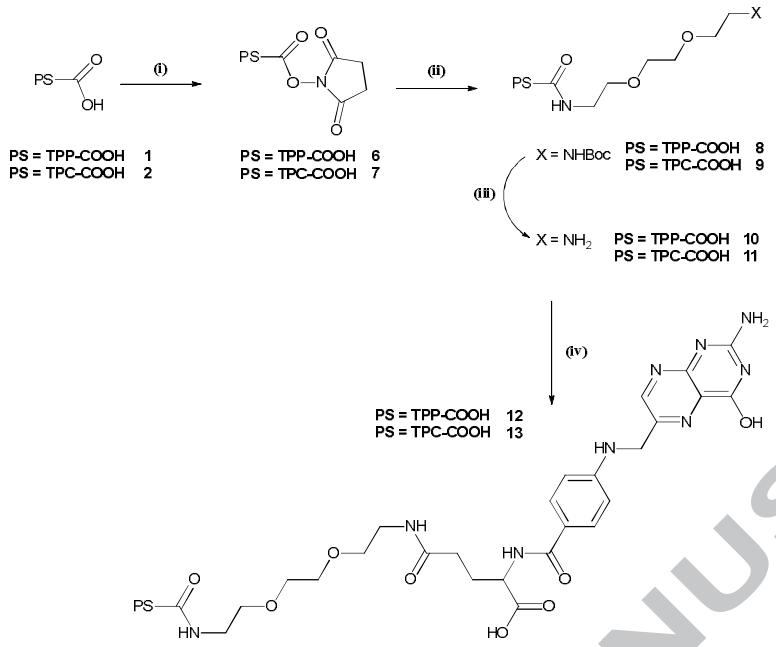

Scheme 1. Synthesis strategy for PS-OEG-FA **12, 13**. (i) NHS, DCC, CH_2Cl_2, 45 °C, overnight. (ii) OEG (*N*-Boc-2,2´-(ethylenedioxy)diethylamine), THF, r.t., 18-24 h. (iii) TFA, r.t., 2h. (iv) FA, DCC, pyridine, DMSO, r.t., 24h

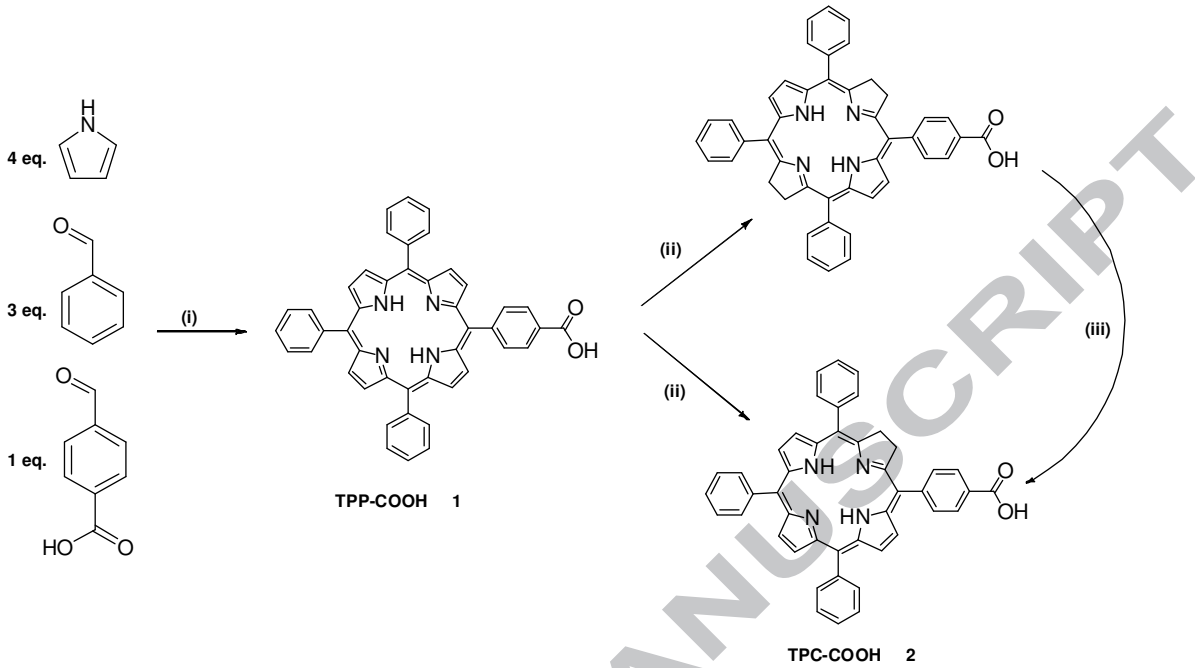

Scheme 2. Synthesis of photosensitizers TPP-COOH **1** and TPC-COOH **2**. (i) $BF_3.(OEt)_2$, CH_2Cl_2, reflux, overnight and then, *p*-chloranil. (ii) *p*-TSH, K_2CO_3, pyridine, reflux, overnight. (iii) EtOAc, *o*-chloranil.

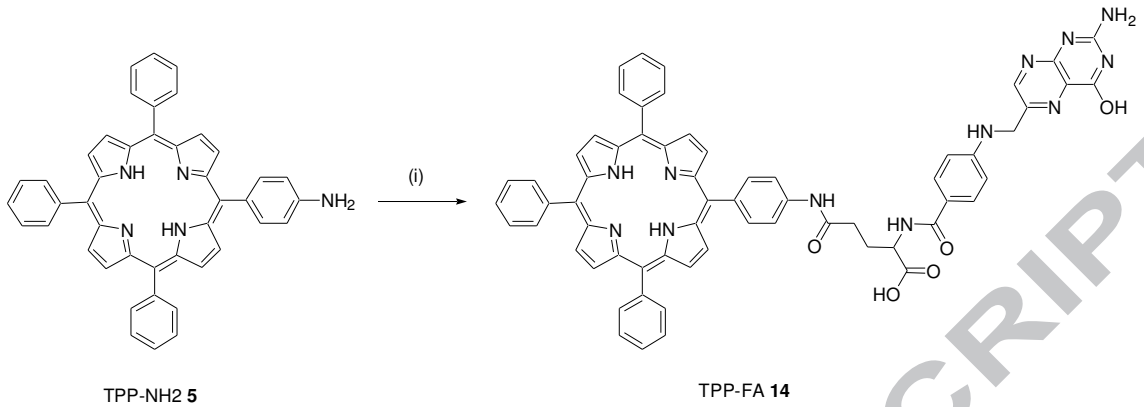

TPP-NH2 **5**

TPP-FA **14**

Scheme 3. Synthesis of TTP-FA **14**: (i) FA, DCC, pyridine, DMSO, r.t., 48h.

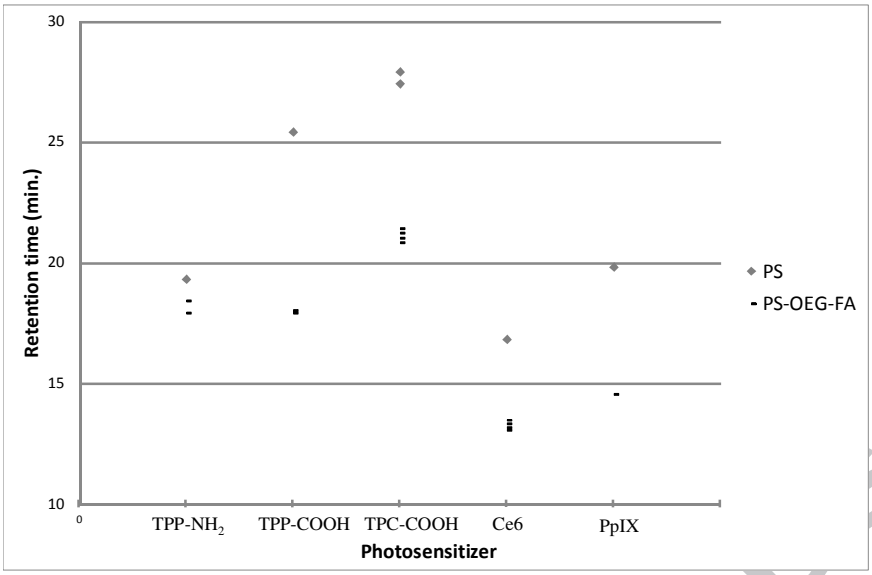

Figure 2. Comparison of the hydrophobicities of PS and FA-targeted PS (reverse phase HPLC (C18 column), acetonitrile/water gradient (10/90 % à 100/0 % in 25 min, 100/0% for 15 min, acetonitrile/water, v/v)). UV-Detection at 415 nm.

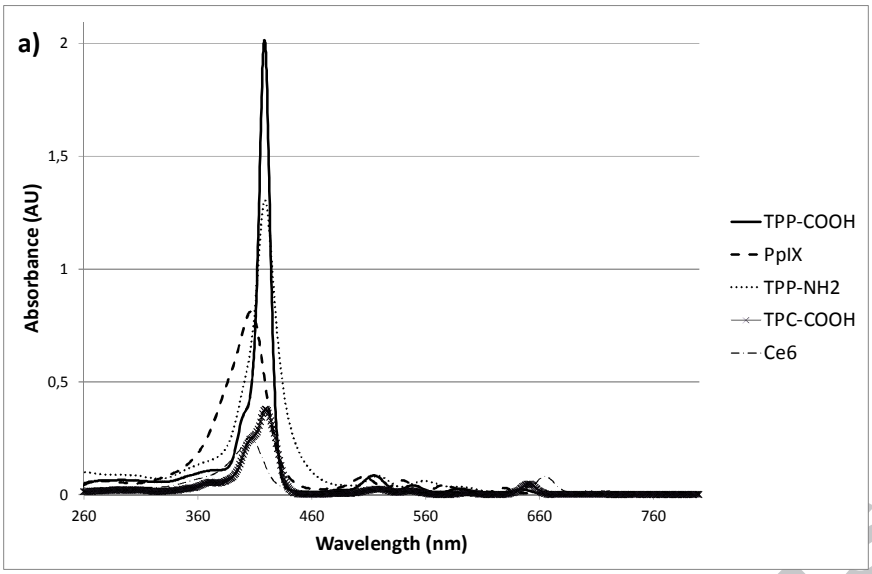

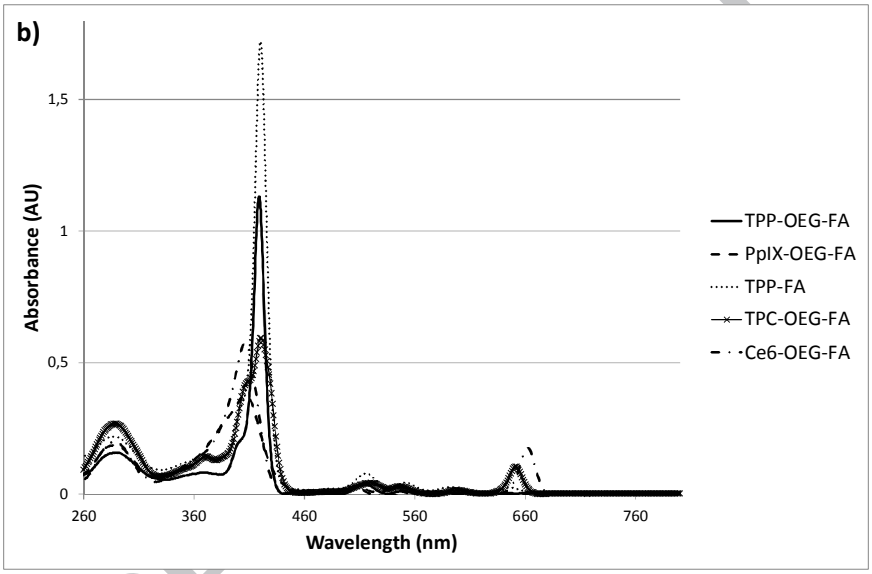

Figure 3. (a) Absorption spectra of photosensitizers in DMSO; (b) Absorption spectra of FA-targeted photosensitizers in DMSO at the same concentration (C= 4.9 E^{-6} M)

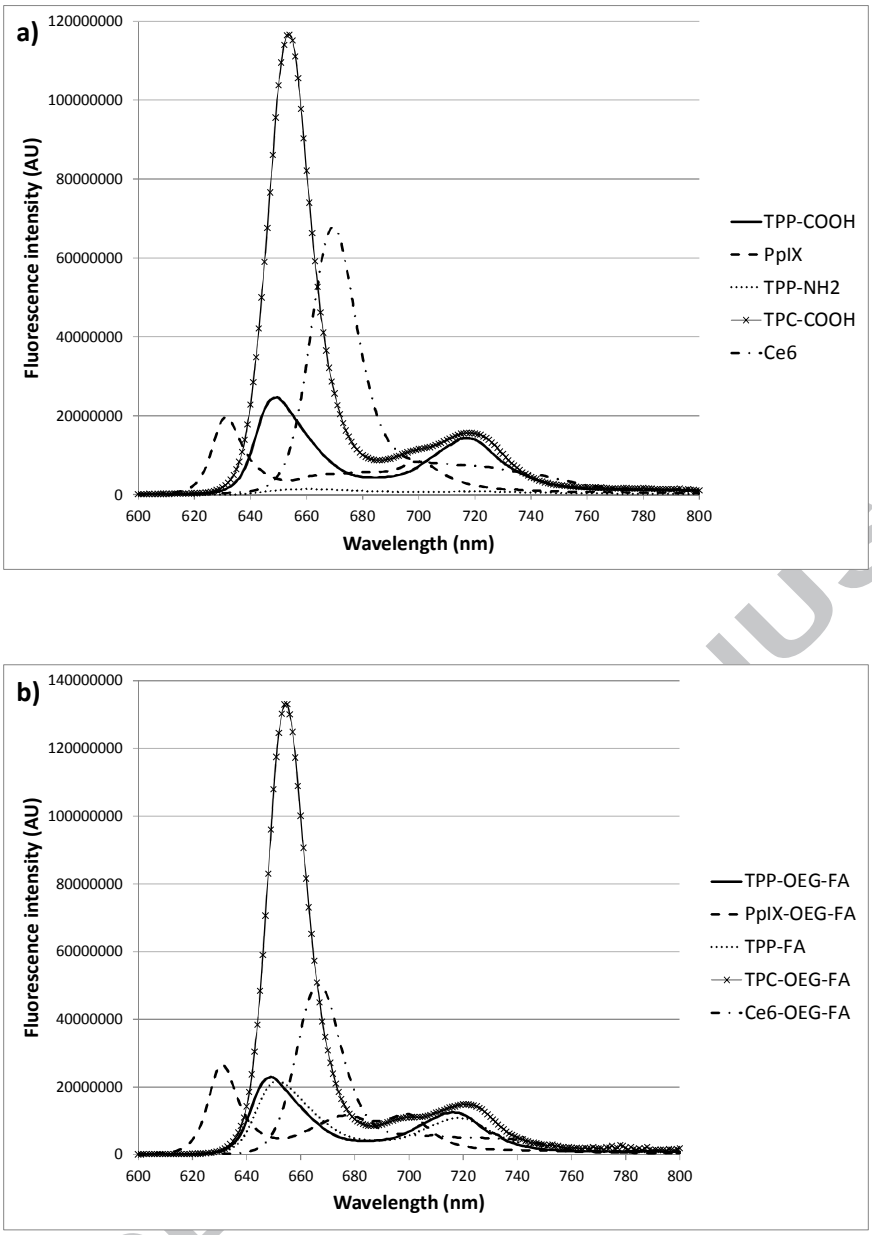

Figure 4. (a) Fluorescence spectra of photosensitizers in DMSO; (b) Fluorescence spectra of FA-targeted photosensitizers in DMSO at the same DO.

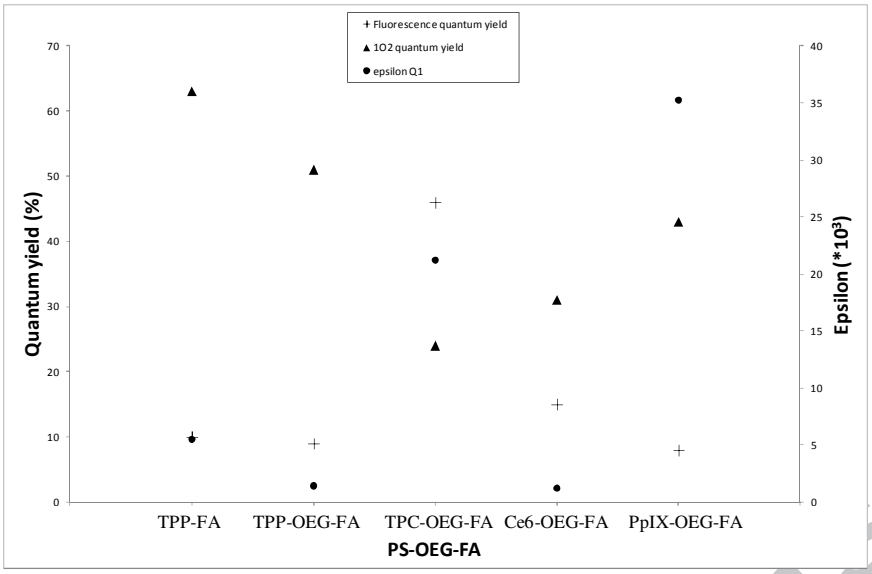

Figure 5. Epsilon of QI, fluorescence quantum yield and singlet oxygen quantum yield of the FA-targeted photosensitizers in DMSO.